

MULTISENSOR DATA FUSION AND FEATURE EXTRACTION FOR FORESTRY APPLICATIONS

Temesgen Gebrie Yitayew, Camilla Brekke, and Anthony P. Doulgeris

Department of Physics and Technology
University of Tromsø, 9037 Tromsø
Norway

ABSTRACT

In this paper we discuss feature level multisensor data fusion with P-, L-, and C-band polarimetric synthetic aperture radar (PolSAR) data and multispectral Landsat Thematic Mapper (TM) data. The application is classification of Maritime pine age classes and bare ground in the Nezer forest in France. Multisensor data fusion is motivated by the complementary information available in SAR and optical data. Our objective is to investigate the choice of features among twenty six well known descriptors. First, we demonstrate the benefit of multisensor data fusion for improved classification performance over single sensor data classification with respect to forest monitoring. A comparison of the classification performances among the four different datasets reveals that the P-band SAR features yield the best results. By combining the P-band SAR features with the multispectral optical features, a significant classification accuracy improvement of 12.6% is achieved. Second, all twenty six features extracted in total from the four datasets are investigated for the purpose of identifying those features jointly possessing the highest discrimination power. Five features are found to preserve 98.5% of the classification information compared to classification based on the total set of features. This shows the advantage of feature selection with respect to preserving classification information while at the same time reducing the dimensionality of the feature space. A potential for improving the classification performance is also found by applying a thorough feature selection procedure.

Index Terms— Polarimetric SAR, Landsat TM, feature selection, data fusion, forest monitoring.

1. INTRODUCTION

In data fusion of multitemporal or multisensor remote sensed data, a challenge lies in the fundamental problem of how to merge the different data sets containing complementary information. The data fusion could take place at the pixel value level, the generated feature level or the classified decision level [1, 2]. *Pixel level fusion* is a low level fusion where different source images are combined to produce a single fused

image. *Feature level fusion* is an intermediate level of fusion that requires the merging of extracted features. *Decision level fusion* is a high level fusion strategy that is used to integrate separately processed image information using decision rules. Feature level fusion might require less memory as compared to pixel level fusion due to a possible reduction of redundant information through a feature selection stage. Extracting and investigating features also allows physical interpretation of the sensor specific parameters and their application relevance. A limitation of data fusion at decision level, i.e. after classification of each sensor dependent data set, is that the fusion process is performed only on discrete class labels (which have lost some detail) and might require ambiguous decision rules. The data fusion strategy discussed in this paper is based on sensor specific feature level fusion.

The aim of this work is to discuss and evaluate PolSAR and multispectral optical features in the context of vegetation classification. The features are fed into a simple maximum likelihood Bayesian classifier, and n -fold cross validation is applied in production of all classification results presented. We study feature based multisensor data fusion of airborne C-, L- and P-band PolSAR data and spaceborne multispectral Landsat TM data over the Nezer forest in France. The application is discrimination of Maritime pine of six different ages and bare soil. Our experiments are based on detailed ground truth information available for this unique data set [3].

Information from the different PolSAR channels represent different characteristics of the observed forest. PolSAR features can be grouped into three categories: i) features processed from the mean covariance matrix [4], ii) textural features based on the data's statistical distribution [4], and iii) features based on various target decomposition theorems [5]. Features from all categories can provide useful physical interpretation of the observed scene, however, only simple features from the first and second categories are considered here to demonstrate the selection technique. For optical data, vegetation indices are the most widely used multispectral features for vegetation applications. They are combinations of two or more bands in a multispectral optical data set. These indices are designed to highlight particular properties of veg-

etation [6]. A comprehensive analysis of a total of twenty six features is presented in this paper.

Section 2 summarizes the preprocessing applied to the data sets. The features extracted are presented and defined in section 3. The experimental results are discussed in section 4 and section 5, and finally the conclusion is given in section 6.

2. DATASET AND PREPROCESSING

The data set consists of three airborne PolSAR images acquired by the NASA/JPL AIRSAR system in August 1989 with three different frequencies, C (5.3 GHz), L (1.2 GHz), and P-band (440 MHz), and one multispectral Landsat TM image recorded in July 1991. The three PolSAR images have four coregistered polarimetric channels (HH, VV, HV, and VH) each and the multispectral image has seven coregistered spectral channels. The resolution of the SAR data is 3×6.7 m and the resolution of the multispectral data is 30×30 m.

The study site consists of Maritime pine trees represented by six different age groups and some bare soil fields. The terrain is flat with no significant slopes. The coverage proportions of each of the different cover classes are as follows (the color coding indicated is applied throughout the paper): Bare soil (yellow) 36.8%, 5-8 years (blue) 7.7%, 8-11 years (cyan) 8.3%, 11-14 years (brick red) 14.2%, 15-19 years (red) 4.1%, 33-41 years (green) 18.9%, and >41 years (forest green) 10.2%. The ground truth map is shown in Fig. 1.

A prerequisite of data fusion is that the data are coregistered, and geometrically and radiometrically corrected [1]. In this study, atmospheric correction is applied to the multispectral Landsat TM data. The multispectral optical image is coregistered with the airborne SAR images by manual image tiepoint selection and resampling, and the SAR images are multilooked to reduce speckle and to adapt to the coarser resolution of the Landsat TM data.

3. FEATURE EXTRACTION

Our classification algorithm is based on feature level fusion. A number of features are extracted at every pixel for each image and listed as a feature vector. Each image may have a different number of extracted features. Hence, a total of k feature vector images, of potentially different lengths, are produced, one for each image. Table 1 presents the twenty six features extracted from the multisensor dataset. This includes six features (μ , f_x , f_c , f_m , f_p , ν) from each of the three SAR data sets (C-, L-, and P-band) and eight from the Landsat TM data set. The foundation of the polarimetric feature extraction can be reviewed in [4]. Theory on the optical features can be found in [6].

4. EXPERIMENT 1: FUSION OF THE DATASETS AND CLASSIFICATION

In the first experiment we have evaluated each of the four datasets (each represented by their entire feature vectors) and

all combinations of these with respect to three different cases:

1. Case #1: Discrimination among bare soil and six different tree age categories.
2. Case #2: Discrimination between bare soil and forest.
3. Case #3: Discrimination among six tree age categories.

The latter case was introduced to eliminate the dominating bare soil class for the purpose of purely studying the sensitivity of the features to different tree age categories. All classification results are computed by averaging ten estimates of the classification accuracy from ten independent training and testing experiments. Classification results are presented in Table 2. Note that the eight extracted Landsat TM features gives a slight improvement in classification accuracy compared to using all Landsat TM bands, except the thermal one, directly. Based on this observation, only extracted features are considered in the following.

Based on a comparison of the whole datasets, P-band PolSAR gives the highest classification performance. We also found that the best performances from the fused datasets involve P-band PolSAR. L-band PolSAR is the second best, followed by multi-spectral optical data, and, finally, C-band PolSAR. C-band PolSAR gives relatively poor performance for forest age classification, nonetheless, it is still expected to be useful for deforestation mapping as it can identify forest versus nonforested areas with reasonable accuracy (see case #2 in Table 2).

From this experiment, we learn that the classification accuracy significantly improves by using a combination of the PolSAR and the multispectral optical data. Note that the results presented in this section are based on *all* the features for a respective dataset. A comparison among the individual features from all datasets follows next.

5. EXPERIMENT 2: INDIVIDUAL FEATURE EVALUATION AND SELECTION

The k feature vectors, one from each dataset, are combined into a concatenated feature vector. This defines the base set for the feature selection procedure. A new ground truth map is created for this experiment, where each class is represented by an equal number of pixels which are randomly picked from the class samples. Thus, the variation in size of the available classes will not influence the feature selection process. The standard sequential forward method (SFFS) is applied. SFFS examines the joint performance of the features while forming different subsets. We use the cross-validation average classification accuracy as a criterion for measuring performance. The joint performance is of interest to demonstrate the benefit of combining different features and will quite naturally avoid highly correlated features. This is due to the fact that if a feature is highly correlated with any of the features in the pre-selected subset, it is more likely that adding it to the subset

Table 1. Extracted features. Landsat TM bands: B_1 blue, B_2 green, B_3 red, B_4 near-IR, B_5 mid-IR, and B_7 mid-IR.

Feature	Definition	Sensor
normalized difference vegetation index	$NDVI = \frac{B_4 - B_3}{B_4 + B_3}$	Landsat TM
brightness, a measure of the soil	$B = \alpha_1 B_1 + \alpha_2 B_2 + \alpha_3 B_3 + \alpha_4 B_4 + \alpha_5 B_5 + \alpha_6 B_7$	Landsat TM
greenness, a measure of the vegetation	$G = \beta_1 B_1 + \beta_2 B_2 + \beta_3 B_3 + \beta_4 B_4 + \beta_5 B_5 + \beta_6 B_7$	Landsat TM
wetness, a measure of interaction of soil and canopy moisture	$W = \gamma_1 B_1 + \gamma_2 B_2 + \gamma_3 B_3 + \gamma_4 B_4 + \gamma_5 B_5 + \gamma_6 B_7$	Landsat TM
perpendicular vegetation index	$PVI = \sqrt{(0.355B_4 - 0.149B_2)^2 + (0.355B_2 - 0.852B_4)^2}$	Landsat TM
triangular vegetation index	$TVI = 0.5(120(B_4 - B_2) - 200(B_3 - B_2))$	Landsat TM
soil adjusted vegetation index	$SAVI = \frac{(1+0.5)(B_4 - B_3)}{(0.5 + B_4 + B_3)}$	Landsat TM
atmospherically resistant vegetation index	$ARVI = \frac{B_4 - (B_3 - 0.3(B_1 - B_3))}{B_4 + (B_3 - 0.3(B_1 - B_3))}$	Landsat TM
mean radar backscatter (μ_P, μ_L, μ_C)	$\mu = \det(C)^{1/d}$	AIRSAR
cross-polarization ratio (f_{xP}, f_{xL}, f_{xC})	$f_x = \frac{2C_{HV}}{C_{HH} + C_{VV}}$	AIRSAR
co-polarization ratio (f_{cP}, f_{cL}, f_{cC})	$f_c = \frac{C_{HH}}{C_{VV}}$	AIRSAR
correlation magnitude (f_{mP}, f_{mL}, f_{mC})	$f_m = \text{mag}(\frac{C_{HHVV}}{\sqrt{C_{HH}C_{VV}}})$	AIRSAR
correlation phase (f_{pP}, f_{pL}, f_{pC})	$f_p = \text{angle}(\frac{C_{HHVV}}{\sqrt{C_{HH}C_{VV}}})$	AIRSAR
non-Gaussianity texture measure (ν_P, ν_L, ν_C)	$\nu = \frac{\text{mean}(x_i^H C^{-1} x_i)^2}{d(d+1)}$	AIRSAR

* α -, β -, and γ -coefficients as defined in [6, p. 387 and references therein].

will add little to the overall performance of the subset. The smallest feature set preserving 95% of the classification accuracy achieved by the total set of twenty six features is finally selected.

Aiming for discrimination between all seven land cover classes, a study based on the SFFS resulted in the selection of four features, which are listed in column one of Table 3. These selected features are now used to perform a classification over the full ground truth image, by randomly selecting an equal number of samples from each class for training. The ground truth image and classification result are shown in the top row of Fig. 1. These four features achieved an overall accuracy of 74.2%. This accounts for 97.7% of the classification accuracy achieved by the complete set of twenty six features, which was 75.9% (see the last line of Table 2).

Next, we eliminate the dominating bare ground class and only focus on discrimination among the six tree age classes. One additional feature, *wetness*, is found useful for tree age discrimination. The five element feature vector is also shown in Table 3. The classification result obtained for the six class tree age problem is shown in the middle row of Fig. 1 and achieved an accuracy of 60.35%. This five element feature vector accounts for 95.7% of the overall classification accuracy achieved by the twenty six features, which was 63.1%.

These five features are also our final selection for the discrimination of all seven landcover classes. The classification result is presented in the last row of Fig. 1. The classification accuracy based on this five element feature vector accounts for 98.5% of the classification accuracy achieved by the complete set of twenty six features.

Table 2. Average classification accuracy (%) and standard deviation for the full feature vectors (datasets) as well as various combinations of the datasets. VI: vegetation index.

Sensor(s) (feature vector length)	Case #1	Case #2	Case #3
SAR, P-band (6)	67.89±0.3	98.94±0.11	49.12±0.45
SAR, L-band (6)	54.76±0.44	98.85±0.21	29.76±0.64
SAR, C-band (6)	43.97±0.94	89.92±0.36	20.70±0.55
Landsat TM VIs (8)	53.34±0.47	91.59±0.37	35.66±1.21
Landsat TM bands (6)	52.07±0.72	-	-
SAR, P and L-band (12)	68.35±0.48	99.30±0.15	49.79±0.52
SAR, P and C-band (12)	68.67±0.43	99.30±0.09	50.03±0.47
SAR, L and C-band (12)	56.63±0.48	99.01±0.21	32.33±0.53
SAR, P, L and C-band (18)	68.9±0.46	99.42±0.11	50.54±0.54
SAR, P-band and 8 VIs (14)	75.34±0.38	99.33±0.17	61.67±0.89
SAR, L-band and 8 VIs (14)	64.82±0.47	97.87±0.73	45.58±0.8
SAR, C-band and 8 VIs (14)	58.19±0.41	93.61±0.50	38.21±1.21
SAR, P, L-band and 8 VIs (20)	75.60±0.39	99.40±0.16	62.44±0.74
SAR, P, C-band and 8 VIs (20)	75.91±0.41	99.42±0.14	62.48±0.82
SAR, L, C-band and 8 VIs (20)	66.13±0.53	98.12±0.67	47.28±0.85
SAR, P, L, C-band and 8 VIs (26)	75.92±0.27	99.46±0.14	63.08±0.66

Table 3. Features selected using SFFS.

Selected features, 7 landcover classes	Selected features, 6 tree age classes
μ_P	μ_P
B	B
$NDVI$	$NDVI$
f_{xP}	f_{xP}
	W

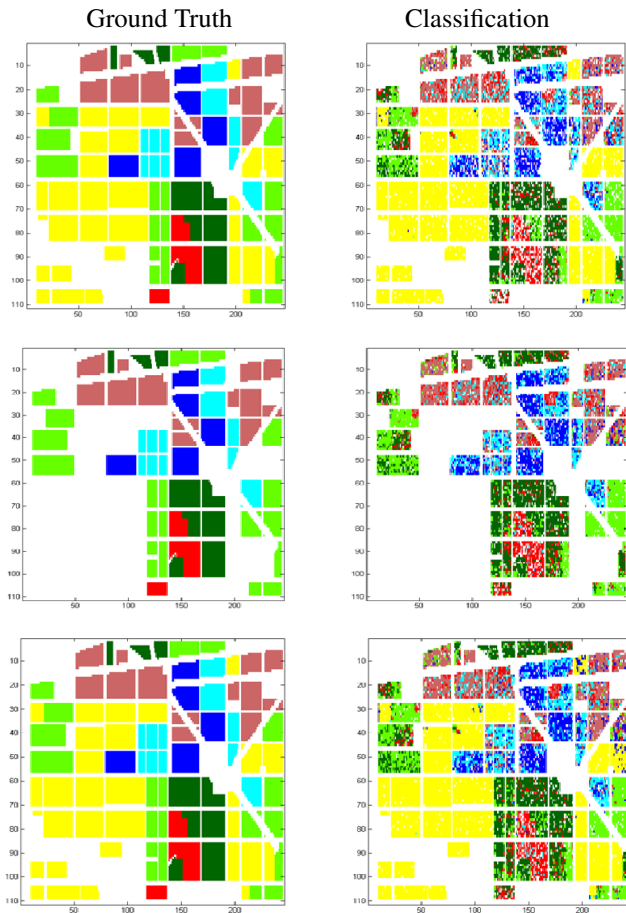


Fig. 1. Columns: ground truth (left), classification results (right). Rows: 7 land cover classes and 4 features (top), 6 land cover classes and 5 features (middle), and 7 land cover classes and 5 features (bottom).

In Table 3, only features from P-band PolSAR and the Landsat TM datasets are represented. Hence, no features are selected from either the L- nor C-band PolSAR measurements. The feature selection experiment was repeated, with one SAR set at a time plus optical, to identify the features performing best independent of the SAR frequency used. We found that the *mean radar backscatter* and the *cross-polarization ratio* of the PolSAR datasets, and the *wetness* and the *brightness* from the Landsat TM dataset are the features that jointly performed best.

6. CONCLUSIONS AND FUTURE WORK

In this study, a total of twenty six features are extracted from remote sensing measurements of forest; six from each of three PolSAR datasets acquired with different frequencies and eight from an optical multispectral dataset. An evaluation of the PolSAR features revealed, as expected, that P-band has better performance than L- and C-band with respect to discrim-

ination power between all the land cover classes investigated (i.e., bare ground and six tree age categories). The L-band PolSAR features and the Landsat TM features provide moderate performances, while the C-band PolSAR features are the poorest. Forest versus nonforest mapping can be accomplished with an accuracy up to 98.9% by utilizing P-band or L-band PolSAR measurements only, or with around 90% using C-band or optical measurements. Hence, no multisensor data fusion is necessary for this task. However, fusion of PolSAR and optical data significantly boosts the discrimination performance between various tree age categories. With little loss of classification performance, five out of twenty six features were selected through a thorough feature selection procedure and recommended for future studies on forest. The five were selected from P-band SAR and Landsat TM only. Future work includes experiments with the selected features on other datasets containing, for example, a mixture of forest tree species, as opposed to the monospecies age discrimination problem considered in this work. We would also consider an investigation of features extracted from PolSAR decompositions, and application of more advanced state-of-the-art classifiers, such as support vector machines, which would improve performance.

7. REFERENCES

- [1] A. H. S. Solberg, "Data fusion for remote sensing applications," *Cp. 11 Image Processing for Remote Sensing*, C. H. Chen (ed.), CRC Press, Taylor and Francis Group, 2008.
- [2] C. Pohl and J. L. Van Genderen, "Multisensor image fusion in remote sensing: concepts, methods and applications," *International Journal of Remote Sensing*, vol. 19, no. 5, pp. 823–854, 1998.
- [3] E. Pottier, J.-S. Lee, and L. Ferro-Famil, "Advanced concepts in polarimetry part 2: Polarimetric target classification.," *Technical report, DTIC Document*, 2005.
- [4] A. P. Doulgeris and T. Eltoft, "Scale mixture of gaussian modelling of polarimetric sar data," *EURASIP Journal on Advances in Signal Processing*, vol. No. 874592, pp. pages 1–12, 2010.
- [5] S. R. Cloude and E. Pottier, "A review of target decomposition theorems in radar polarimetry.," *IEEE Transactions on Geoscience and Remote Sensing*, vol. 32(2), pp. 498–518, 1996.
- [6] J. R. Jensen, "Remote sensing of the environment. an earth resource perspective (2 edition)," *Prentice Hall Series in Geographic Information Science*, Clarke, K. C. (ed.), 2007.